This is the accepted manuscript (postprint) of the following article:
R. Amini, E. Salahinejad, M. Hadianfard, M. Marasi, T. Sritharan, *Characterization of Fe–Cr–Mn–N amorphous powders with a wide supercooled liquid region developed by mechanical alloying*, Materials Science and Engineering: A, 527 (2010) 1135-1142.
https://doi.org/10.1016/j.msea.2009.09.061

Characterization of Fe–Cr–Mn–N amorphous powders with a wide supercooled liquid region developed by mechanical alloying

R. Amini [a, b *], E. Salahinejad [a], M. J. Hadianfard [a], M. Marasi [a], T. Sritharan [b]

[a] Department of Materials Science and Engineering, School of Engineering, Shiraz University, Zand Blvd., 7134851154, Shiraz, Iran

[b] School of Materials Science and Engineering, Nanyang Technological University, Block N4.1, 50 Nanyang Avenue, 639798, Singapore

Abstract

In the present study, amorphous Fe–18Cr–4Mn–*x*N alloys were successfully synthesized by mechanical alloying (MA) of pure elemental powders under a nitrogen gas atmosphere. The microstructure of the milled products at different stages of milling was characterized by X-ray diffraction (XRD) and high-resolution transmission electron microscopy (TEM). Furthermore, differential scanning calorimetry (DSC) was conducted to investigate the thermal stability and to determine the glass formation ability and the crystallization behavior of the amorphous as-milled powders. The results showed that by increasing the milling time, the amorphous phase content increases and after 126 h the amorphization process becomes complete. The alloys exhibited a distinct glass transition and a wide supercooled liquid region that increased by increasing the milling time. It was found

* *Corresponding author. e-mail: ramini2002@gmail.com*

This is the accepted manuscript (postprint) of the following article:
R. Amini, E. Salahinejad, M. Hadianfard, M. Marasi, T. Sritharan, *Characterization of Fe–Cr–Mn–N amorphous powders with a wide supercooled liquid region developed by mechanical alloying*, Materials Science and Engineering: A, 527 (2010) 1135-1142.
https://doi.org/10.1016/j.msea.2009.09.061

out that dissolved nitrogen atoms play a crucial role in the amorphization and the exhibition of the large supercooled liquid region.

Keywords: Amorphous Fe–Cr–Mn–N alloys; Supercooled liquid region; Transmission electron microscopy (TEM); X-ray diffraction (XRD); Differential scanning calorimetry (DSC)

1. Introduction

Recently, there has been considerable interest in synthesizing amorphous materials to obtain superior properties. Amorphous alloys with a large glass formation ability are a novel class of engineering materials due to their exceptional mechanical properties and relatively high corrosion resistance [1-3]. This new type of materials allows for the production of large-scale bulk amorphous materials [2-6]. Furthermore, alloys with a wide supercooled liquid state are expected to be formed into bulk materials with various shapes and dimensions through considerable viscous flow inherent to the supercooled liquid [6-8].

Although the majority of amorphous alloys are conventionally produced by melt-quenching techniques, mechanical alloying (MA) is a good alternative method to synthesize these alloys [2-5,9-13]. This method is one of the most promising and rapidly developing solid-state processing routes to produce non-equilibrium and metastable phases [14-16]. MA has been successfully employed to fabricate several metallic amorphous alloys that cannot be readily accessible by conventional processes [2-4,17-20]. Several reports on the successful formation of single and homogeneous amorphous phase through MA have been published [4,5,21,22]. This technique proposes the possibility of the formation of bulk amorphous materials through powder metallurgy route and subsequent consolidation. In order to avoid

This is the accepted manuscript (postprint) of the following article:
R. Amini, E. Salahinejad, M. Hadianfard, M. Marasi, T. Sritharan, *Characterization of Fe–Cr–Mn–N amorphous powders with a wide supercooled liquid region developed by mechanical alloying*, Materials Science and Engineering: A, 527 (2010) 1135-1142.
https://doi.org/10.1016/j.msea.2009.09.061

the oxidation of the powder samples, MA has normally been performed under an inert gas atmosphere like argon. However, MA under a reactive gas atmosphere, such as nitrogen has been employed to produce an amorphous phase [4,5,22-29] and crystalline compounds [30-34] through an solid-gas reaction.

Multi-component Fe–Cr–Mn–N alloys are a new class of engineering materials with superior mechanical properties and good corrosion resistance [34-38], which can be improved significantly by progression of an amorphous phase in these alloys. The production of these materials with an amorphous structure in the powder and bulk forms can release a new field of knowledge in the development of these novel materials. The effect of nitrogen content on the thermal behavior and micro-indentation response of single-phase amorphous Fe–18Cr–4Mn–*x*N powders prepared by MA has been assessed, in which thermal evaluations have been conducted only to determine the supercooled liquid region [22]. Nitrogen incorporation, grain refinement, and phase transformations occurring during MA of Fe–18Cr–8Mn–*x*N alloys have been also studied [23]. In the latter paper, fully amorphous alloys were not obtained by the employed high-energy shaker mill. In addition, concise thermal studies have been performed to confirm the production of an amorphous phase during MA. Moreover, the effect of structure on magnetic properties of as-milled and heat-treated Fe–18Cr–12Mn–*x*N samples has been investigated [24].

The main aim of this work is the evaluation of thermal properties of mechanically alloyed Fe–18Cr–4Mn–*x*N powders in detail. For this purpose, microstructural evolutions during MA under reactive and non-reactive atmospheres are also studied. Thermal studies including the glass formation ability, crystallization behavior, and kinetics of these events are conducted for the partially and fully amorphous powders.

This is the accepted manuscript (postprint) of the following article:
R. Amini, E. Salahinejad, M. Hadianfard, M. Marasi, T. Sritharan, *Characterization of Fe–Cr–Mn–N amorphous powders with a wide supercooled liquid region developed by mechanical alloying*, Materials Science and Engineering: A, 527 (2010) 1135-1142.
https://doi.org/10.1016/j.msea.2009.09.061

2. Experimental procedure

In the present study, different grades of nitrogen-containing Fe–18Cr–4Mn alloys were processed by the ball milling process of pure elemental Fe (Merck, >99.5%, $D_{a.v.}$ = 50 μm), Cr (Merck, >99.9%, $D_{a.v.}$ = 150 μm), and Mn (Merck, >99.9%, $D_{a.v.}$ = 50 μm) powders under a pressurized nitrogen gas atmosphere. The milling process was performed in the Fritsch planetary ball mill by using a tempered steel bowl (V = 630 cm^3) and balls (d = 8 mm). The rotation speed of 250 rpm and the ball-to-powder mass ratio of 20:1 were used for this purpose. The ball milling process was interrupted at 18-hour intervals for powders sampling. The process was considered complete when the X-ray diffractometer pattern consisted of a single diffuse peak associated with an amorphous phase. In order to study the effect of the milling atmosphere on the amorphization process during MA, the ball milling process was also performed under an argon atmosphere by the same procedure.

The phase constituent and structural properties of the powders were investigated by powder X-ray diffraction (XRD, SHIMADZU Lab X-6000, Cu Kα radiation) and high-resolution transmission electron microscopy (HRTEM, JEOL, JEM 2010). The glass transition and crystallization behavior of the samples were investigated by using a differential scanning calorimetry (DSC, NETZSCH, STA 449C Jupiter) with an alumina container under a flowing purified argon gas. Prior to the DSC analyses, the powders were compacted by a uniaxial compession method and the bulk samples were prepared for testing. In order to confirm the reproducibility of the results, at least three DSC examinations were carried out on each sample. Also, the chemical composition of the as-milled powders was determined by X-

This is the accepted manuscript (postprint) of the following article:
R. Amini, E. Salahinejad, M. Hadianfard, M. Marasi, T. Sritharan, *Characterization of Fe–Cr–Mn–N amorphous powders with a wide supercooled liquid region developed by mechanical alloying*, Materials Science and Engineering: A, 527 (2010) 1135-1142.
https://doi.org/10.1016/j.msea.2009.09.061

ray fluorescence (XRF, PHILIPS, PW2400) and LECO TC 436 and CS 600 (LECO Corp., St. Joseph, MI) gas analyzers.

3. Results

3.1. Chemical composition

Table 1 shows the chemical composition of the samples obtained after various milling times. The results indicate that the expected nominal composition of Fe–18Cr–4Mn was achieved and the only detectable impurity in the as-milled powders is oxygen which can be due to the natural oxidation of the powders in the atmosphere. It is obvious that for the samples milled under the nitrogen atmosphere, the total nitrogen content steadily increases almost linearly from 0.55 to 3.62 wt.% when the milling time increases from 18 to 144 h. This implies that during MA under the nitrogen atmosphere as a result of solid-gas reactions a high quantity of nitrogen atoms has been diffused into the structure of the powders.

3.2. Microstructure

3.2.1. XRD analysis

Fig. 1 depicts the phase development in terms of XRD patterns obtained at the proper stages of milling during MA of the elemental Fe, Cr, and Mn powders. The XRD pattern of the sample after 18 h of MA comprises the major peaks of ferrite (α) and austenite (γ) phases. By progression of the MA process, the peaks related to the α-phase become considerably broad, and the γ-phase becomes dominant. After 54 h of the ball milling peocess, the only detectable crystalline phase is austenite (fcc). The interpretation of the XRD data by the TOPAS software version 3, suggests that the fcc phase is nanocrystalline with an average

This is the accepted manuscript (postprint) of the following article:
R. Amini, E. Salahinejad, M. Hadianfard, M. Marasi, T. Sritharan, *Characterization of Fe–Cr–Mn–N amorphous powders with a wide supercooled liquid region developed by mechanical alloying*, Materials Science and Engineering: A, 527 (2010) 1135-1142.
https://doi.org/10.1016/j.msea.2009.09.061

grain size of 8 nm and a lattice parameter of 3.63 Å, which conforms well with austenitic stainless steels. Therefore, it is obvious that MA in the present ball-milling schedule has been successful in synthesizing the nanocrystalline stainless steel powders with the fcc crystal structure. This also provides evidence that MA of elemental Fe, Cr, and Mn powders under the nitrogen gas atmosphere has resulted in the structural transformation of bcc to fcc through the dissolution of Cr, Mn, and N in a solid state to develop the austenitic stainless steel. More focus on the XRD results (Fig. 1) demonstrates that by progression of the MA process the broadening of the first-order maxima corresponding to the (111) reflection is increased and the peaks related to higher order reflections gradually disappear. The XRD profile of the sample obtained after 72 h of milling illustrates a large broadening in the first-order maxima. This can be due to the presence of a significant amount of amorphous phase in the microstructure. However, the presence of the detectable intensity peak corresponding to the (200) reflection indicates the presence of a considerable amount of the crystalline phases along with the amorphous phase. The Bragg peaks related to the high-order reflections (2θ higher than 50^{o}) completely disappear after 90 h of milling and by the further continuation of milling (126 h) the sharpness of the broad peak disappears gradually and it becomes rounded, leading to the complete amorphization. At this stage, the system has reached a steady state and the XRD patterns did not change obviously by the further extension of the milling time.

With the aim of determining the effects of nitrogen on the amorphization process, the same ball milling procedure was applied to the elemental powders under the argon atmosphere. Fig. 2 illustrates the XRD profiles of the powders under the argon and nitrogen gas atmospheres after a prolonged milling process (144 h). Obviously, in the powders milled under the argon atmosphere the structure contains the crystalline α-phase. Also, according to the broadening of the first-order peak ((111) reflection), the amorphous phase might be presented in a small quantity. However, in the powders milled under the nitrogen atmosphere the only detectable phase is the amorphous phase. Therefore, in the present case, it can be inferred that the presence of nitrogen are essential for the α-to-γ phase transformation and the amorphization during MA.

3.2.2. TEM observations

Fig. 3 presents the HRTEM image and the correlated selected area diffraction (SAD) pattern of the as-milled powders at the different ball milling intervals. As it appeared from the image and the bright vague rings of the SAD pattern of Fig. 3-(a), at a short milling time (18 h) the nanocrystalline ferrite and austenite phases are the dominant structure. By progression of the MA process to 72 h, the quantity of amorphous phase increases and the corresponding TEM image (Fig. 3-(b)) shows the presence of the crystalline regions within a featureless amorphous matrix. Also, the related SAD pattern indicates the diffraction spots arising out of the crystalline regions along with the halo pattern due to the amorphous phase present in the matrix. Further milling leads to the synthesization of the fully amorphous phase with a homogeneous fine structure, as indicated in Fig. 3-(c). The observation is corroborated by the clear appearance of the halo in the resultant SAD pattern. The above-mentioned results have a good agreement with the XRD results mentioned in the previous section.

Fig. 4 shows the HRTEM image and the SAD pattern of the alloyed powder after 144 h of milling under the argon gas atmosphere. This reveals that the structure contains a predominant nanocrystalline α-phase. The corresponding SAD pattern shows the rings arising out of the nanocrystalline regions along with the trivial diffuse halo on the first bright ring due to the presence of the amorphous phase in a small amount. By comparing the image of Figs. 4 and 3-(c), it can be concluded that the milling atmosphere plays an important role in the amorphization process.

3.3. Glass formation ability and crystallization behavior

3.3.1. Milling under the nitrogen atmosphere

In order to determine the thermal stability of the alloyed powders, differential scanning calorimetry (DSC) was conducted at a constant heating rate of 20 K/min under the argon gas atmosphere (Fig. 5). All the samples were heated up to 1000 K (first run) and cooled down to about 400 K. Then, the second heating runs were performed to establish the base line. As it appears from Fig. 5, all of the powders except the one milled for 18 h reveal a significantly broad endothermic event with a very wide temperature span reflecting the heat capacity anomaly characteristic of the glass transition. At higher temperatures, an exothermic peak indicating the successive stepwise transformation from a supercooled liquid state to a crystalline phase is exhibited. Furthermore, for the short milling times (lower than 90 h) an exothermic event appeared at temperature ranges from 656 to 695 K. In order to determine the origin of these reactions, the DSC test was carried out again on the as-milled samples in the same manner and the samples were heated up to the temperatures well below and above the temperature ranges of the reactions in the DSC curve. Subsequently, the XRD analyses were performed on these samples at room temperature. Since the sample milled for 54 h clearly indicates the first exothermic peak and since the sample milled for 144 h obviously shows the endothermic event and the second exothermic peak, these sets of experiments were performed on these samples (Fig. 6). Apparently, the first exothermic peak in the DSC curve

This is the accepted manuscript (postprint) of the following article:
R. Amini, E. Salahinejad, M. Hadianfard, M. Marasi, T. Sritharan, *Characterization of Fe–Cr–Mn–N amorphous powders with a wide supercooled liquid region developed by mechanical alloying*, Materials Science and Engineering: A, 527 (2010) 1135-1142.
https://doi.org/10.1016/j.msea.2009.09.061

at around 676 K corresponds to the structural transformation from the *γ*-phase (fcc) to *α*-phase (bcc), as seen in Fig. 6-(a). As the milling time increases, the ratio of the crystalline-to-amorphous phase content decreases and consequently this peak begins to vanish in the DSC curve. Furthemore, the XRD analyses of the samples taken just above the endothermic events of the DSC curve do not show a significant structural change of the material and no evidence for crystallization is found, whereas the samples annealed far above the exothermic reaction show the formation of a crystalline ferrite and the CrN and Cr_2N phases (Fig. 6-(b)). Fig. 5 clearly indicates that as the milling time increases, the crystallization peak moves to the high temperature side, becoming more pronounced and sharp. This indicates that the amorphous phase quantity and homogeneity increase by progression of the MA process. After 126 h, the crystallization temperature and the heat of crystallization are, no longer, changed obviously, demonstrating that the milling-induced amorphization approaches a steady state. The glass transition and crystallization temperatures (T_g and T_x) were defined as the onset temperatures of the endothermic and exothermic DSC events, respectively. The exact amount of these temperatures is listed in Table 2. According to these data, the stability range of supercooling liquid region (SLR) (T_x-T_g) increased by increasing the milling time, reaching 92 K for the sample milled for 144 h.

In order to increase the evidence for the amorphicity of the alloys, the isothermal DSC scan was also performed on the sample milled for 144 h under the nitrogen atmosphere (Fig. 7). The signals exhibit the typical bell shape related to the first-order phase transition associated with the formation and growth of nuclei. This confirms unambiguously that the high-temperature exothermic events in Fig. 5 are related to the crystallization of the amorphous phase and not to the grain growth phenomenon of the nanocrystalline material.

This is the accepted manuscript (postprint) of the following article:
R. Amini, E. Salahinejad, M. Hadianfard, M. Marasi, T. Sritharan, *Characterization of Fe–Cr–Mn–N amorphous powders with a wide supercooled liquid region developed by mechanical alloying*, Materials Science and Engineering: A, 527 (2010) 1135-1142.
https://doi.org/10.1016/j.msea.2009.09.061

With the purpose of determining the stability of the amorphous phase as well as the kinetics behavior of the glass transition and crystallization events, further DSC experiments were carried out at different heating rates (C) of 10, 20, 30, 40, and 50 K/min on the powders milled for 144 h. Based on Fig. 8, by increasing the heating rate, both T_g and T_x are shifted to higher temperatures, thereby signifying that not only the crystallization temperature but also the glass transition temperature of the amorphous powders behave in a markedly kinetics manner. Fig. 9 shows that T_g and T_x have a linear relationship with ln$C$, which is compatible with the Lasocka's equation [39] ($T_g = A + B \ln C$, $T_x = M + N \ln C$). The values of A, B, M, and N, which can be determined by the slopes of these curves are listed in the Table 3. One of the important characteristics of the thermal transition process is the activation energy for the glass transition (E_g) and crystallization (E_a) that can be determined by the Kissinger's equation as follows [40]:

$$\ln\left(\frac{C}{T_p^{\,2}}\right) = -\frac{E_a}{RT_p} + const. \tag{1}$$

$$\ln\left(\frac{C}{T_g^{\,2}}\right) = -\frac{E_g}{RT_g} + const. \tag{2}$$

where T_p and T_g are the crystallization peak and glass transition temperatures, respectively. Also, C is the heating rate and R is the gas constant. Fig. 10-(a) depicts the linear relationship between ln (C/T_p^2) and ($1/T_p$). Also, the same relation between ln (C/T_g^2) and ($1/T_g$) is present in Fig. 10-(b). The values of E_a and E_g can be easily determined by the slopes of these curves as shown in the Fig. 10 and Table 3. According to the above-mentioned experimental results, the glass transition and crystallization of the amorphous powders can be considered to be kinetically modified thermodynamic phase transformation processes. This also shows that by increasing the milling time the stability of the amorphous phase as well as the liquid phase

This is the accepted manuscript (postprint) of the following article:
R. Amini, E. Salahinejad, M. Hadianfard, M. Marasi, T. Sritharan, *Characterization of Fe–Cr–Mn–N amorphous powders with a wide supercooled liquid region developed by mechanical alloying*, Materials Science and Engineering: A, 527 (2010) 1135-1142.
https://doi.org/10.1016/j.msea.2009.09.061

region increase along with the growth in the effective activation energy of the glass transition and crystallization.

3.3.2. Milling under the argon atmosphere

Fig. 11 compares the DSC results of the powders milled for 144 h under the argon and nitrogen gas atmospheres. As it is observable, the DSC trace of the sample milled under the argon gas contains a broad exothermic event corresponding to the crystallization of the amorphous phase which is available in a small amount along with the crystalline compounds. In addition, no glass transition is detectable in this DSC curve. Accordingly, it can be concluded that without using nitrogen as the atmosphere of milling, the amorphization process is diminished dramatically and the glass transition does not occur during the heating of the as-milled powders.

4. Discussion

4.1. Amorphization

MA of the elemental Fe, Cr, and Mn powders under the argon gas atmosphere yields the bcc solid solution along with a small amount of the amorphous phase. In contrast, the achievement of the fully amorphized structure is possible by MA in the presence of the nitrogen gas atmosphere. This shows that the nitrogen atoms play an essential role in the amorphization process. The concentration of the nitrogen atoms infused during MA increases with increasing the milling time, approaching 3.62 wt.% after 144 h of milling. At an early stage of milling, due to the severe plastic deformation of the powder particles, the preferred

This is the accepted manuscript (postprint) of the following article:
R. Amini, E. Salahinejad, M. Hadianfard, M. Marasi, T. Sritharan, *Characterization of Fe–Cr–Mn–N amorphous powders with a wide supercooled liquid region developed by mechanical alloying*, Materials Science and Engineering: A, 527 (2010) 1135-1142.
https://doi.org/10.1016/j.msea.2009.09.061

crystallographic orientations are developed and by continuing the milling process the crystallites become randomly oriented and the grain size begins to decrease [23-26].

During MA under the nitrogen gas atmosphere, the incorporated nitrogen atoms apparently lead to the expansion of the lattice and the creation of strain in the crystallites. This strain energy can be reduced in the elastic field of dislocations and grain boundaries. Consequently, the diffused nitrogen atoms which were adsorbed on the newly created surfaces of the powder particles will penetrate into the particles by diffusing down to the dislocations and grain boundaries. Then, the nitrogen atoms are segregated into the grain boundaries, resulting in the formation of the stable alloy with a high amount of nitrogen [23-25]. Furthermore, the trickling down of running dislocations from the body of the grains on dislocations which are fixed by the diffusion of the nitrogen atoms leads to the creation of nuclei for new boundaries [41]. This provides a nanometer structure with a very small crystallite size to the order of a few nanometers. As a result of increasing the constraints from the neighboring grains, the grain boundary structure itself will become unstable with decreasing the grain size. It was reported that when the average grain size decreases to about 5 nm, the grain boundary will be transformed into the amorphous phase [26]. Moreover, the absorption of the nitrogen atoms is influenced by the atomic-size effect and the chemical affinities with the parent atoms. Since the atomic size effect is less in the amorphous phase than the grain boundary and is less in the grain boundary than the crystalline lattice [25], from this point of view, the thermodynamic stability of the amorphous phase is higher than the grain boundary and that of the grain boundary is higher than the crystallite. This reveals that for the progressive dissolution of the nitrogen atoms in the structure, the grain refinement and subsequently the amorphization are required. At a sufficiently high concentration of nitrogen atoms, the amorphous phase grows and consumes the crystalline lattice and the amorphization process will be completed unless nitride phases, such as Cr_2N or CrN are formed. In the absence of any solute source, e.g. where elemental powders are milled in an argon atmosphere, grain refinement also occurs but not to the same extent as in the nitrogen atmosphere and under these conditions, full amorphization does not occur.

In addition to the aforementioned reasons for the amorphization, intermixing at atomic levels is another important cause of amorphization. It was reported that the intermixing of the constituent elements of iron and nitrogen did not fully occur on an atomic scale during MA [13]. It reveals that other constituents like chromium and manganese are essential to achieve the fully amorphized structure. Hence, it appears that when Cr and Mn with high affinity for N are added to Fe–N alloys, the intermixing of the atomic species Fe, Cr, Mn, and N readily occurs at an atomic level, resulting in the formation of the amorphous phase. In order to evaluate the effects of the Cr and Mn on the amorphization of Fe–N materials thermodynamically, the values of the interaction parameters of Cr and Mn with N atoms (W_{CrN} and W_{MnN}) proposed by Miura et al. [13] were used. The interaction parameter represents the difference between the bonding energy of the Cr–N and Fe–N (U_{CrN}-U_{FeN}) atomic pairs and that of the Mn–N and Fe–N (U_{MnN}-U_{FeN}) pairs in the ternary Fe–Cr–N and Fe–Mn–N solutions, respectively. The quantities of $W_{Cr\text{-}N}$ and $W_{Mn\text{-}N}$ are -332 and -104 kJ mol^{-1}, respectively. As it can be seen, both of them are negative but the absolute value of $W_{Cr\text{-}N}$ is higher, which demonstrates the stronger interaction and bonding between Cr and N. With the negative interaction parameters, the mixing enthalpy of the system is negative and the formation of the ternary Fe–Cr–N and Fe–Mn–N solutions results in decreasing the free energy of the system. In other words, the addition of such elements to the Fe–N alloy provides a thermodynamic driving force for the formation of the ternary solution, and the intermixing of the constituent atoms becomes easier. Alternatively, due to the strong interaction between these atoms and N, the activity of nitrogen decreases, prohibiting the diffusion of nitrogen over a large distance during MA [13]. This retards the recovery processes like the nucleation and/or growth of more stable phases, such as the formation of nitrides, which participates with the amorphization reaction in the MA process.

Meanwhile, during MA, the powder particles are subjected to severe plastic deformation and extreme cold working. This increases the dislocation density in the structure to the considerably high levels. In such a case, the pipe diffusion through dislocation cores becomes the dominant mode of the diffusion changing from the normal lattice diffusion mode [10]. As the local temperature increases to a high level in the MA process, the value of diffusion (through dislocation cores) can be improved to high levels, approaching the values of the lattice diffusion at close-to-melting temperatures [10]. This high atomic mobility can enhance the formation of an amorphous phase. It should be noticed that in the present case as the structure of the powders milled for a prolonged time under the argon atmosphere is predominantly a nanocrystalline phase rather than the amorphous phase, the direct effect of cold work on amorphization is minor. However, as the dissolved nitrogen increased by increasing the density of dislocations, the indirect effect of the cold working on the amorphization process of the powders milled under the nitrogen atmosphere is considerable.

4.2. Glass formation and crystallization

MA of the elemental Fe, Cr, and Mn powder mixture under the nitrogen atmosphere leads to the synthesis of the amorphous alloy with a wide supercooled liquid region (SLR). In contrast, milling under the argon atmosphere results in the partial amorphization without any detectable SLR. There exist different aspects explaining this phenomenon. Inoue et al. [42] suggested that large atomic size ratios and attractive bonding nature between the main constituent elements, together with the difficulty of the redistribution of these elements for crystallization are the dominant factors of the increase in the glass formation ability and the appearance of a wide SLR. With respect to the atomic radius of Fe (0.126 nm), Cr (0.128 nm), and Mn (0.127 nm), it can be concluded that in the absence of nitrogen, the first parameter (large atomic size ratios) is not an important factor in the Fe–Cr–Mn system. Furthermore, these three elements are close to each other in the periodic table and their heat of mixing is not considerable, revealing that the metallic bondings are not the main source of the large SLR. As a result, the presence of nitrogen is essential to obtain the wide SLR. It can be inferred that the appearance of the extended supercooled liquid region before crystallization is mainly due to the difficulty of the redistribution of nitrogen for the crystallization and the requirement of large chemical fluctuations to form the critical nuclei of crystalline phases from the homogeneous amorphous phase. In addition, owing to the high affinity of the constituent elements (especially chromium) for nitrogen, there is a strong bonding energy between each of these elements with nitrogen, which increases the glass formation ability and the width of SLR. This conclusion is supported by the negative mixing enthalpy of these elements with nitrogen atoms. It should be mentioned that by progression of the MA process, the glass transition and crystallization temperatures rise, signifying the stability improvement of the amorphous phase and SLR. This is due to an increase in the homogeneity of the amorphous phase as well as the amount of dissolved nitrogen in the

This is the accepted manuscript (postprint) of the following article:
R. Amini, E. Salahinejad, M. Hadianfard, M. Marasi, T. Sritharan, *Characterization of Fe–Cr–Mn–N amorphous powders with a wide supercooled liquid region developed by mechanical alloying*, Materials Science and Engineering: A, 527 (2010) 1135-1142.
https://doi.org/10.1016/j.msea.2009.09.061

microstructure, delaying the glass formation and crystallization events according to the aforementioned explanations.

5. Conclusions

The present study has shown that a homogeneous amorphous phase with a wide supercooled liquid region (SLR) can be synthesized by the reactive mechanical alloying (MA) of the elemental Fe, Cr, and Mn powder mixtures with the nominal composition of 78Fe–18Cr–4Mn (wt.%) under a nitrogen gas atmosphere. This study has also revealed that during the milling process in an inert atmosphere like argon, the structure contains a predominant nanocrystalline ferrite phase and a trivial amount of amorphous phase. The implication is that the atmosphere of milling plays an essential role in the phase transformation and the amorphization process during MA of the Fe–Cr–Mn alloys. During the milling process under the nitrogen gas atmosphere, the nitrogen atoms are infused into and subsequently dissolved in the structure of the powder particles and act as the main source of the amorphization process. The dissolution of 3.45 wt.% N resulted in the complete amorphization of the solid solution after 126 h of milling. The amorphous powders were found to exhibit a glass transition with a wide supercooled liquid region (SLR) of 92 K before the crystallization process. This allows for the production of bulk amorphous Fe–Cr–Mn–N alloys for technical applications, provided that the amorphous powders are consolidated with suitable techniques. The stability of the amorphous phase and the width of SLR were increased by increasing the quantity of the dissolved nitrogen as well as the homogeneity of the amorphous phase. This shows the potential of the reactive MA process as a versatile method to synthesize the amorphous Fe–Cr–Mn–N alloys with the high stability and the extended SLR. It was also found out that the glass transition and crystallization of the amorphous powders can be considered to be kinetically modified thermodynamic phase transformation processes.

6. Acknowledgments

Shiraz University Research Council and Nanyang Technological University (NTU) are also acknowledged due to their support for this study.

References

[1] H.S. Chen, Glassy metals, Rep. Prog. Phys. 43 (1980) 353-432.

[2] X.Q. Zhang, E. Ma, J. Xu, Mechanically alloyed multi-component Mo-based amorphous alloys with wide supercooled liquid region, J. Non-Cryst. Solids 352 (2006) 3985-3994.

[3] P.Y. Lee, C.K. Lin, I.K. Jeng, C.C. Wang, G.S. Chen, Characterization of $Ni_{57}Zr_{20}Ti_{18}Al_5$ amorphous powder obtained by mechanical alloying, Mater. Chem. Phys. 84 (2004) 358-362.

[4] M. Seidel, J. Eckert, L. Schultz, Mechanically alloyed Zr–Ti–Cu–Ni amorphous alloys with significant supercooled liquid region, Mater. Lett. 23 (1995) 299-304.

[5] H. Miura, S. Isa, K. Omuro, Preparation of Fe–Ni-based metal-metalloid amorphous alloys by mechanical alloying and mechanical grinding methods, Jpn. J. Appl. Phys., Part 1, 29 (1990) 339-342.

[6] A. Peker, W.L. Johnson, A highly processable metallic glass: $Zr_{41.2}Ti_{13.8}Cu_{12.5}Ni_{10.0}Be_{22.5}$, Appl. Phys. Lett. 63 (1993) 2342-2344.

[7] Y. Kawamura, H. Kato, A. Inoue, T. Masumoto, Full strength compacts by extrusion of glassy metal powder at the supercooled liquid state, Appl. Phys. Lett. 67 (1995) 2008- 2010.

[8] M.H. Lee, D.H. Bae, W.T. Kim, D.H. Kim, E. Rozhkova, P.B. Wheelock, D.J. Sordelet, Synthesis of Ni-based bulk amorphous alloys by warm extrusion of amorphous powders, J. Non-Cryst. Solids 315 (2003) 89-96.

[9] C.J. Hu, P.Y. Lee, Formation of Cu–Zr–Ni amorphous powders with significant supercooled liquid region by mechanical alloying technique, Mater. Chem. Phys. 74 (2002) 13-18.

[10] R. Sundaresan, A.G. Jackson, S. Krishnamurthy, F.H. Froes, Study of the formation of the amorphous phase in metallic systems by mechanical alloying, Mater. Sci. Eng. 97 (1988) 115-119.

[11] P.P. Chattopadhyay, A. Samanta, W. Lojkowski, H.J. Fecht, I. Manna, Microstructure/phase evolution in mechanical alloying/milling of stainless steel and aluminum powder blends, Metall. Mater. Trans. A 38A (2007) 2298-2307.

[12] K. Aoki, A. Memezawa, T. Masumoto, Nitrogen-induced amorphization of Ti–Zr powders during mechanical alloying, Appl. Phys. Lett. 61 (9) (1992) 1037-1039.

[13] H. Miura, K. Omuro, H. Ogawa, Preparation of amorphous high nitrogen iron alloys with ternary additions by mechanical alloying, ISIJ Int. 36 (1996) 951-957.

[14] C. Suryanarayana, Mechanical alloying and milling, Prog. Mater. Sci. 46 (2001) 1-184.

[15] M. Sherif El-Eskandarany, S. Ishihara, W. Zhang, A. Inoue, Fabrication and characterizations of new glassy $Co_{71}Ti_{24}B_5$ alloy powders and subsequent hot pressing into a fully dense bulk glass, Metall. Mater. Trans. 36A (2005) 141-147.

[16] T. Eckert, L. Schultz, K. Urban, Formation of quasicrystals by mechanical alloying, Appl. Phys. Lett. 55 (1989) 117-119.

[17] S. Suriñach, J.J. Suñol, M.D. Baró, Preparation of Fe–Ni based metal-metalloid amorphous powders by mechanical alloying, Mater. Sci. Eng. A181-182 (1994) 1285-1290.

[18] R. Schwarz, C.C. Koch, Formation of amorphous alloys by the mechanical alloying of crystalline powders of pure metals and powders of intermetallics, Appl. Phys. Lett. 49 (1986) 146-148.

[19] K. Suzuki, A structural study of the solid state vitrification of metals and oxides by ball milling, J. Non-Cryst. Solids 112 (1989) 23-32.

[20] M. Sherif El-Eskandarany, K. Aoki, K. Suzuki, Formation of amorphous aluminum tantalum nitride powders by mechanical alloying, Appl. Phys. Lett. 60 (1992) 1562-1563.

[21] H.M. Wu, S.S. Hung, P.Y. Lee, Characterization of $Ni_{57}Zr_{20}Ti_{20}Sn_3$ amorphous powders obtained by mechanical alloying, J. Alloys Compd. 434-435 (2007) 386-389.

[22] E. Salahinejad, R. Amini, M. Marasi, T. Sritharan, M.J. Hadianfard, The effect of nitrogen on the glass-forming ability and micro-hardness of Fe–Cr–Mn–N amorphous alloys prepared by mechanical alloying, Mater. Chem. Phys. doi: 10.1016/j.matchemphys.2009.07.005.

[23] R. Amini, M.J. Hadianfard, E. Salahinejad, M. Marasi, T. Sritharan, Microstructural phase evaluation of high-nitrogen Fe–Cr–Mn alloy powders synthesized by the mechanical alloying process, J. Mater. Sci. 44 (2009) 136-148.

[24] R. Amini, H. Shokrollahi, E. Salahinejad, M.J. Hadianfard, M. Marasi, T. Sritharan, Microstructural, thermal and magnetic properties of amorphous/nanocrystalline FeCrMnN alloys prepared by mechanical alloying and subsequent heat treatment, J. Alloys Compd. 480 (2009) 617-624.

[25] Y. Ogino, S. Murayama, Y. Yamazaki, Influence of milling atmosphere on amorphization of chromium and Cr-Cu powders by ball milling, J. Less-Common Met. 168 (1991) 221-235.

[26] Y. Ogino, T. Yamasaki, S. Murayama, R. Sakai, Non-equilibrium phases formed by mechanical alloying of Cr–Cu alloys, J. Non-Cryst. Solids 117-118 (1990) 737-740.

[27] T. Fukunaga, E. Ishikawa, T. Koyano, U. Mizutani, Nitrogen induced amorphization observed by neutron diffraction in the Cr–Fe system, Physica B 213-214 (1995) 526-528.

[28] T. Fukunaga, N. Kuroda, C.H. Lee, T. Koyano, U. Mizutani, Nitrogen induced amorphization observed by X-ray and neutron diffractions in the immiscible V–Cu system, J. Non-Cryst. Solids 176 (1994) 98-103.

[29] K. Aoki, A. Memezawa, T. Masumoto, Amorphization of Ti–Zr powders by mechanical alloying in H_2, N_2 and O_2 atmospheres, Mater. Sci. Eng. A181-182 (1994) 1263-1267.

[30] J.C. Rawers, D. Govier, R. Doan, Nitrogen addition to iron powder by mechanical alloying, Mater. Sci. Eng. A 220 (1996) 162-167.

[31] M. Méndez, H. Mancha, M.M. Cisneros, G. Mendoza, J.I. Escalante, H.F. López, Structure of a Fe–Cr–Mn–MovN alloy processed by mechanical alloying, Metall. Mater. Trans. A 33 (2002) 3273-3278.

[32] D. Shaham, J. Rawers, E. Zolotoyabko, Structural transformation of iron powders mechanically processed in nitrogen, Mater. Lett. 27 (1996) 41-45.

[33] A. Munitz, G. Kimmel, J.C. Rawers, R.J. Fields, Ball milling induced bct phase formation in iron and iron alloys, Nanostruct. Mater. 8 (1997) 867-877.

[34] M.M. Cisneros, H.F. López, H. Mancha, D. Vázquez, E. Valdés, G. Mendoza, M. Méndez, Development of austenitic nanostructures in high-nitrogen steel powders processed by mechanical alloying, Metall. Mater. Trans. A 33 (2002) 2139-2144.

[35] N. Nakada, N. Hirakawa, T. Tsuchiyama, S.Takaki, Grain refinement of nickel-free high nitrogen austenitic stainless steel by reversion of eutectoid structure, Script. Mater. 57 (2007) 153-156.

[36] M. Sumita, T. Hanawa, S.H. Teoh, Development of nitrogen-containing nickel-free austenitic stainless steels for metallic biomaterials–review, Mater. Sci. Eng. C 24 (2004) 753-760.

[37] G. Balachandran, M.L. Bhatia, N.B. Ballal, P.K. Rao, Some theoretical aspects on designing nickel free high nitrogen austenitic stainless steels, ISIJ Int. 41 (2001) 1018-1027.

[38] S. Fréchard, A. Redjaïmia, E. Lach, A. Lichtenberger, Dynamical behaviour and microstructural evolution of a nitrogen-alloyed austenitic stainless steel, Mater. Sci. Eng. A 480 (2008) 89-95.

[39] M. Lasocka, The effect of scanning rate on glass transition temperature of splat-cooled $Te_{85}Ge_{15}$, Mater. Sci. Eng. 23 (1976) 173-177.

[40] H.E. Kissinger, Reaction kinetics in differential thermal analysis, Anal. Chem. 29 (1957) 1702-1706.

[41] E.P. Yelsukov, G.A. Dorofeev, A.V. Zagainov, N.F. Vildanova, A.N. Maratkanova, Initial stage of mechanical alloying in the Fe–C system, Mater. Sci. Eng. A 369 (2004) 16-22.

[42] A. Inoue, T. Zhang, T. Masumoto, Glass-forming ability of alloys, J. Non-Cryst. Solids 156-158 (1993) 473-480.

This is the accepted manuscript (postprint) of the following article:
R. Amini, E. Salahinejad, M. Hadianfard, M. Marasi, T. Sritharan, *Characterization of Fe–Cr–Mn–N amorphous powders with a wide supercooled liquid region developed by mechanical alloying*, Materials Science and Engineering: A, 527 (2010) 1135-1142.
https://doi.org/10.1016/j.msea.2009.09.061

Figures:

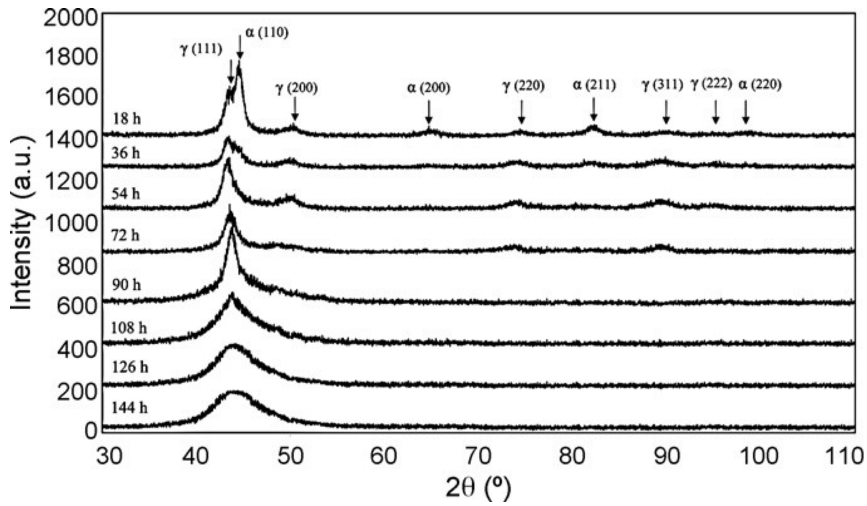

Fig. 1. The XRD pattern of the powders milled for various times under the nitrogen atmosphere.

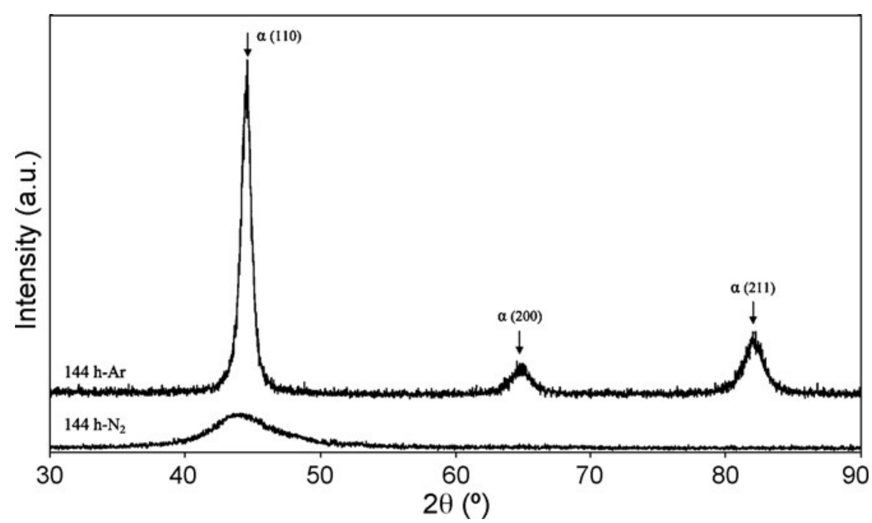

Fig. 2. Comparing the XRD pattern of the powders milled for 144 h under the nitrogen and argon atmospheres.

This is the accepted manuscript (postprint) of the following article:
R. Amini, E. Salahinejad, M. Hadianfard, M. Marasi, T. Sritharan, *Characterization of Fe–Cr–Mn–N amorphous powders with a wide supercooled liquid region developed by mechanical alloying*, Materials Science and Engineering: A, 527 (2010) 1135-1142.
https://doi.org/10.1016/j.msea.2009.09.061

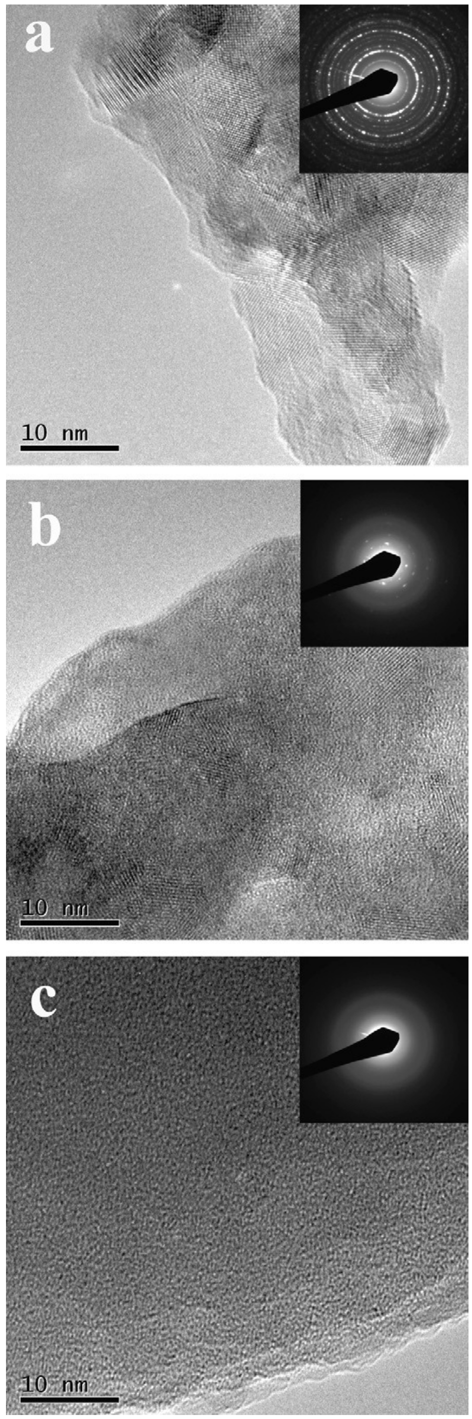

Fig. 3. HRTEM micrographs of the powder particles milled under the nitrogen atmosphere

for (a) 18 h (b) 72 h (c) 126 h.

This is the accepted manuscript (postprint) of the following article:
R. Amini, E. Salahinejad, M. Hadianfard, M. Marasi, T. Sritharan, *Characterization of Fe–Cr–Mn–N amorphous powders with a wide supercooled liquid region developed by mechanical alloying*, Materials Science and Engineering: A, 527 (2010) 1135-1142.
https://doi.org/10.1016/j.msea.2009.09.061

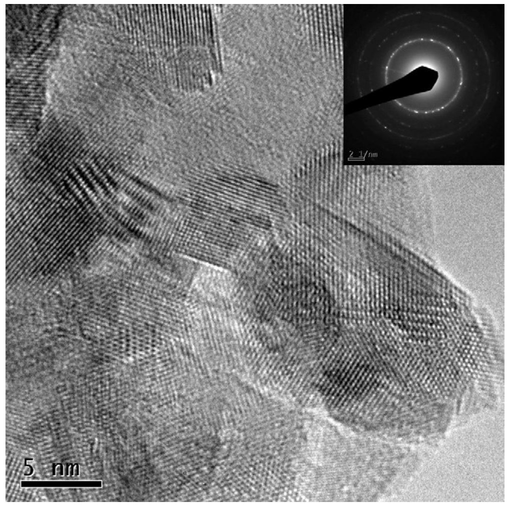

Fig. 4. The HRTEM micrographs of the powder particles milled under the argon atmosphere for 144 h.

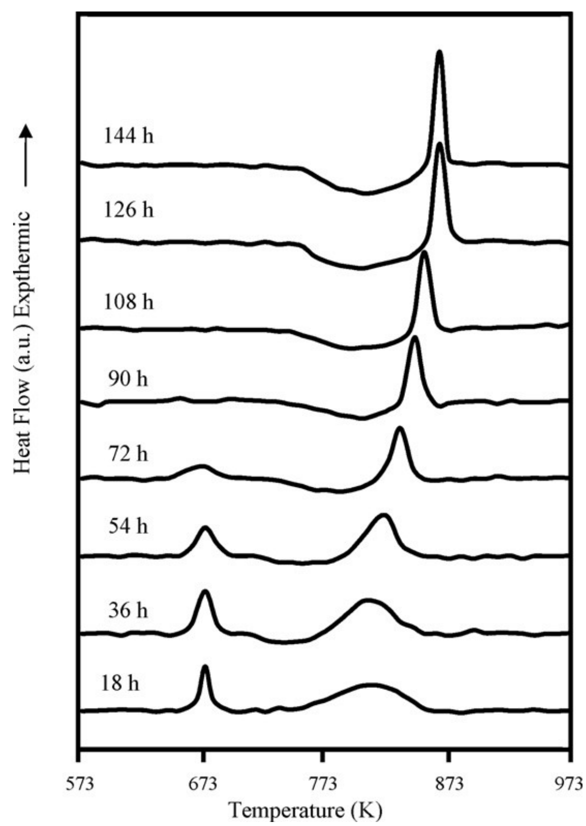

Fig. 5. The DSC profile of the samples milled under the nitrogen atmosphere.

This is the accepted manuscript (postprint) of the following article:
R. Amini, E. Salahinejad, M. Hadianfard, M. Marasi, T. Sritharan, *Characterization of Fe–Cr–Mn–N amorphous powders with a wide supercooled liquid region developed by mechanical alloying*, Materials Science and Engineering: A, 527 (2010) 1135-1142.
https://doi.org/10.1016/j.msea.2009.09.061

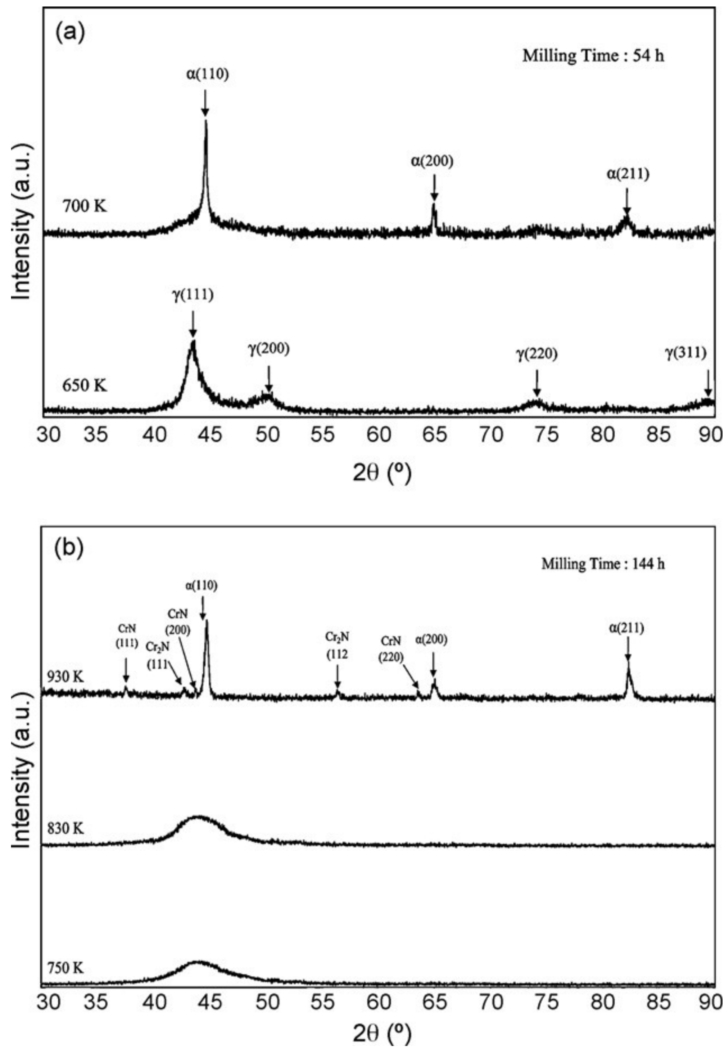

Fig. 6. The XRD pattern of the samples milled under the nitrogen atmosphere (a) 54 h, after DSC test at 650 and 700 K (b)144 h, after DSC test at 750, 830, and 930 K.

This is the accepted manuscript (postprint) of the following article:
R. Amini, E. Salahinejad, M. Hadianfard, M. Marasi, T. Sritharan, *Characterization of Fe–Cr–Mn–N amorphous powders with a wide supercooled liquid region developed by mechanical alloying*, Materials Science and Engineering: A, 527 (2010) 1135-1142.
https://doi.org/10.1016/j.msea.2009.09.061

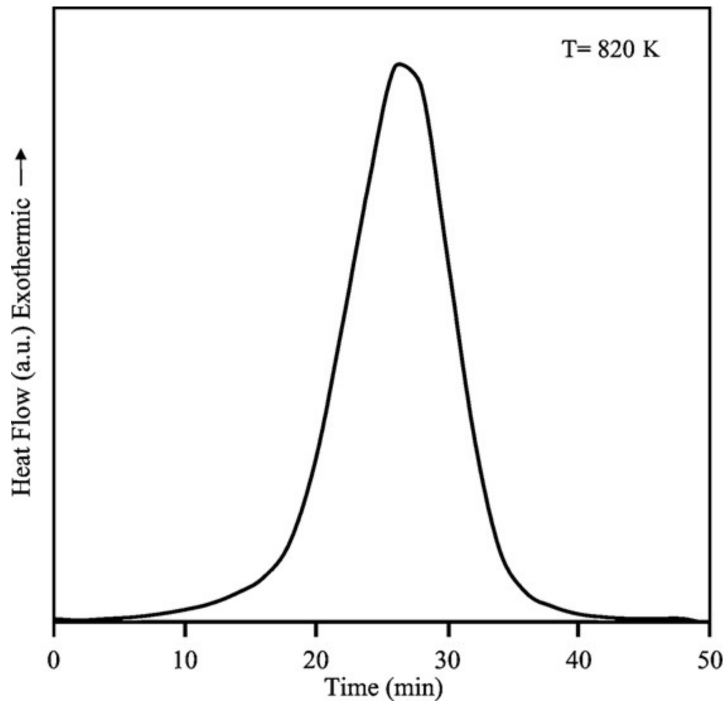

Fig. 7. The isothermal DSC test performed on the sample milled for 144 h under the nitrogen atmosphere .

This is the accepted manuscript (postprint) of the following article:
R. Amini, E. Salahinejad, M. Hadianfard, M. Marasi, T. Sritharan, *Characterization of Fe–Cr–Mn–N amorphous powders with a wide supercooled liquid region developed by mechanical alloying*, Materials Science and Engineering: A, 527 (2010) 1135-1142.
https://doi.org/10.1016/j.msea.2009.09.061

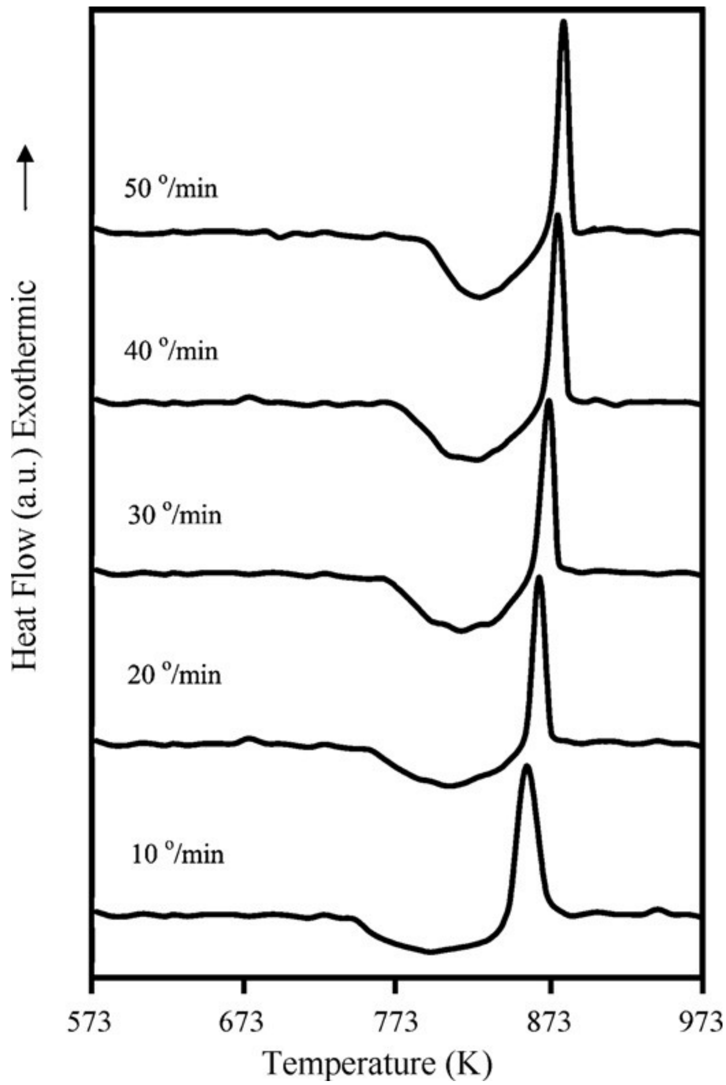

Fig. 8. The DSC profile of the samples milled for 144 h at the different heating rates.

This is the accepted manuscript (postprint) of the following article:
R. Amini, E. Salahinejad, M. Hadianfard, M. Marasi, T. Sritharan, *Characterization of Fe–Cr–Mn–N amorphous powders with a wide supercooled liquid region developed by mechanical alloying*, Materials Science and Engineering: A, 527 (2010) 1135-1142.
https://doi.org/10.1016/j.msea.2009.09.061

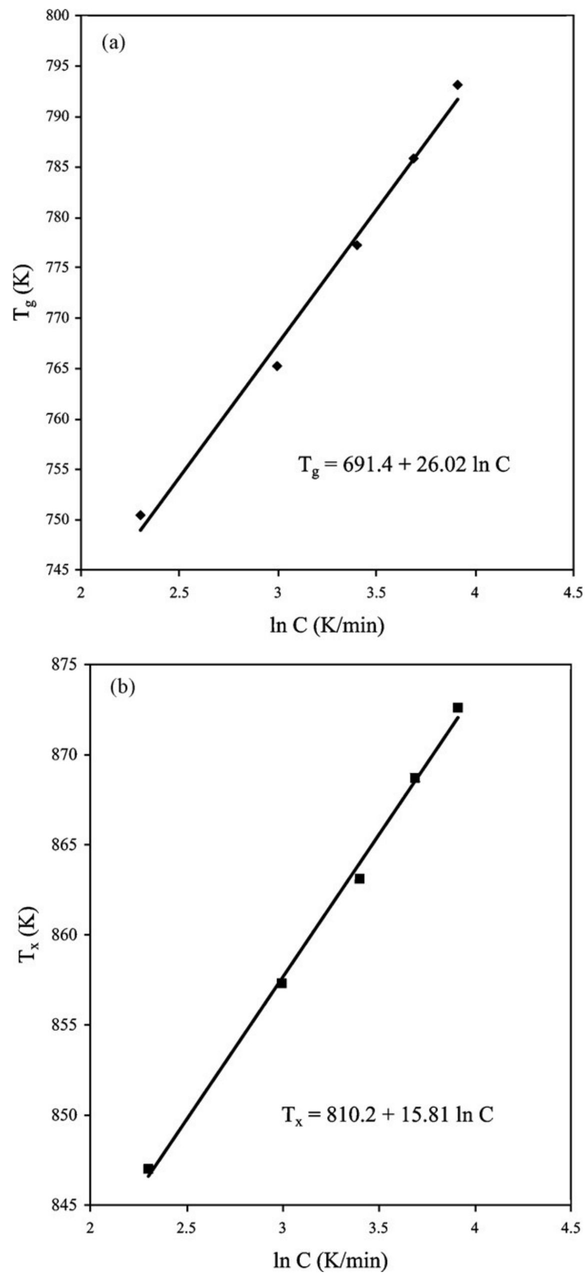

Fig. 9. The Lasocka's plot of the samples milled for 144 h (a) T_g (b) T_x.

This is the accepted manuscript (postprint) of the following article:
R. Amini, E. Salahinejad, M. Hadianfard, M. Marasi, T. Sritharan, *Characterization of Fe–Cr–Mn–N amorphous powders with a wide supercooled liquid region developed by mechanical alloying*, Materials Science and Engineering: A, 527 (2010) 1135-1142.
https://doi.org/10.1016/j.msea.2009.09.061

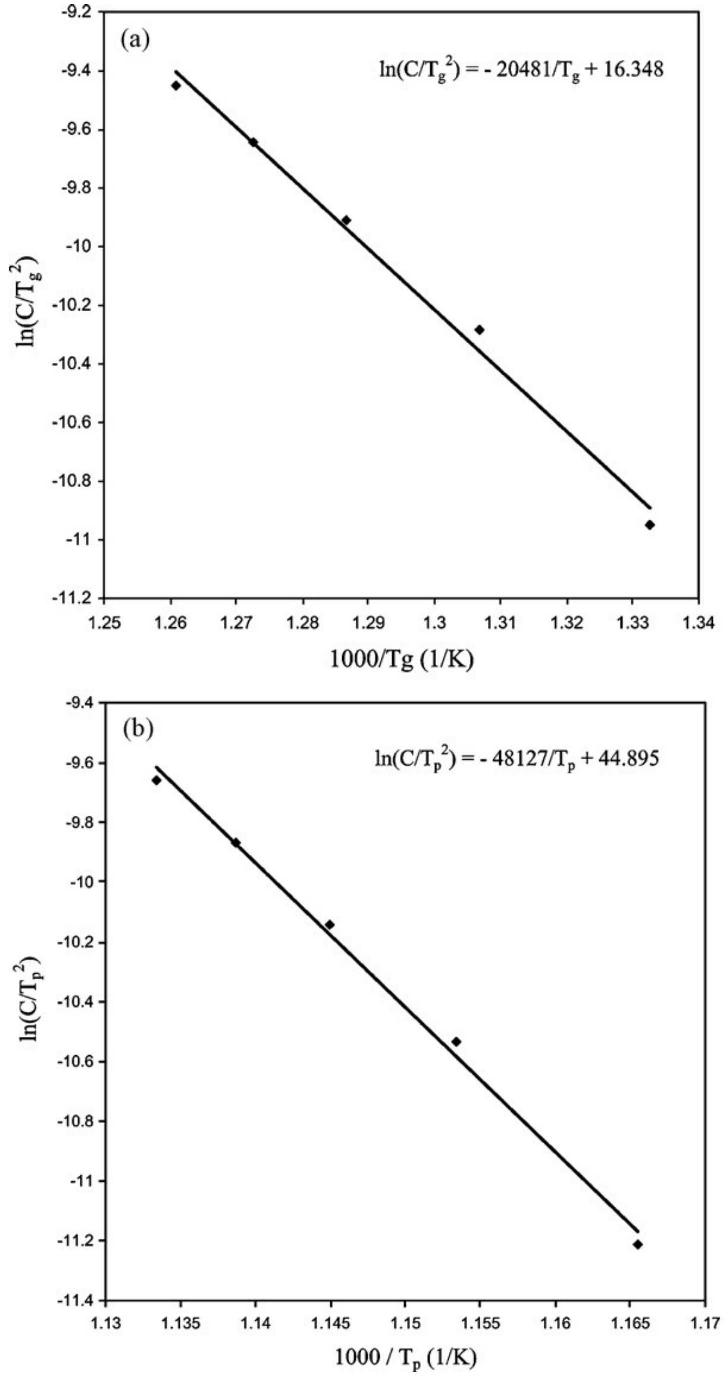

Fig. 10. The Kissinger's plots of the samples milled for 144 h (a) T_g (b) T_p.

This is the accepted manuscript (postprint) of the following article:
R. Amini, E. Salahinejad, M. Hadianfard, M. Marasi, T. Sritharan, *Characterization of Fe–Cr–Mn–N amorphous powders with a wide supercooled liquid region developed by mechanical alloying*, Materials Science and Engineering: A, 527 (2010) 1135-1142.
https://doi.org/10.1016/j.msea.2009.09.061

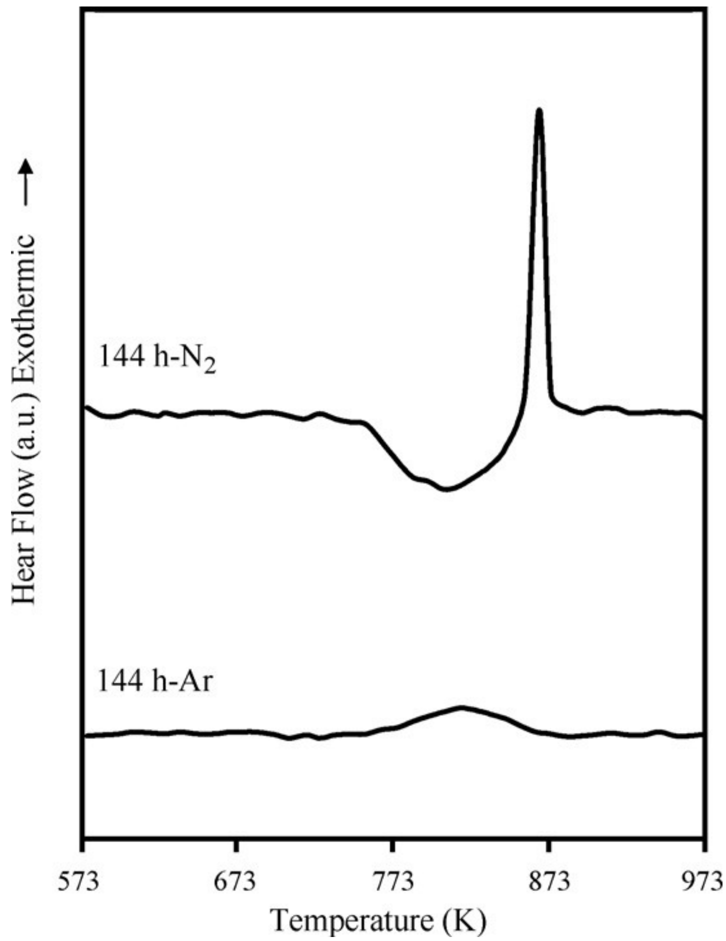

Fig. 11. Comparing the DSC profile of the samples milled for 144 h under the nitrogen and argon atmospheres.

This is the accepted manuscript (postprint) of the following article:
R. Amini, E. Salahinejad, M. Hadianfard, M. Marasi, T. Sritharan, *Characterization of Fe–Cr–Mn–N amorphous powders with a wide supercooled liquid region developed by mechanical alloying*, Materials Science and Engineering: A, 527 (2010) 1135-1142.
https://doi.org/10.1016/j.msea.2009.09.061

Tables:

Table 1. The chemical composition of the powders milled under the nitrogen and argon atmospheres after the different milling times

Milling Atmosphere	Milling Time (h)	Concentration (wt.%)					
		Fe	Cr	Mn	N	O	C
N_2	18	77.514	17.770	3.826	0.55	0.31	0.030
	36	77.550	17.688	3.690	0.74	0.30	0.032
	54	77.397	17.438	3.634	1.19	0.31	0.031
	72	77.243	17.318	3.500	1.57	0.34	0.029
	90	76.783	17.197	3.430	2.27	0.29	0.030
	108	76.451	17.073	3.337	2.81	0.30	0.029
	126	75.833	17.034	3.335	3.45	0.32	0.028
	144	75.541	17.038	3.471	3.62	0.30	0.030
Ar	18	77.704	17.786	4.091	0.06	0.33	0.029
	36	77.760	17.661	4.129	0.07	0.35	0.030
	54	77.801	17.620	4.119	0.08	0.35	0.030
	72	77.914	17.555	4.100	0.08	0.32	0.031
	90	77.865	17.495	4.147	0.10	0.36	0.033
	108	78.091	17.448	4.041	0.09	0.30	0.030
	126	78.099	17.419	4.071	0.07	0.31	0.031
	144	78.070	17.397	4.111	0.05	0.34	0.032

Table 2. The variation of T_g, T_x, and SLR with the milling time

Milling Time (h)	T_g (K)	T_x (K)	SLR (T_x-T_g) (K)
18	-	755	-
36	716	762	46
54	726	785	60
72	735	805	70
90	745	824	79
108	755	841	86
126	764	855	91
144	765	857	92

This is the accepted manuscript (postprint) of the following article:
R. Amini, E. Salahinejad, M. Hadianfard, M. Marasi, T. Sritharan, *Characterization of Fe–Cr–Mn–N amorphous powders with a wide supercooled liquid region developed by mechanical alloying*, Materials Science and Engineering: A, 527 (2010) 1135-1142.
https://doi.org/10.1016/j.msea.2009.09.061

Table 3. The Lasocka's equation constants (*A*, *B*, *M*, and *N*) and the activation energy of glass transition (E_g) and crystallization (E_a) of the samples milled for 144 h

A	691.40
B	26.02
M	810.20
N	15.81
E_a (kJmol^{-1})	400.13
E_g (kJmol^{-1})	170.28